Electronic supplementary Information for

Immobilizing cobalt phthalocyanine into porous carbonized wood membrane as a self-supported heterogenous electrode for selective and stable CO_2 electroreduction in water

Haidong Zhang,[a,b,c] Shixiong Min, *[a,b,c] Fang Wang,[a,b,c] and Zhengguo Zhang[a,b,c]

[a] School of Chemistry and Chemical Engineering, Key Laboratory of Electrochemical Energy Conversion Technology and Application, North Minzu University, Yinchuan, 750021, P. R. China.

[b] Key Laboratory of Chemical Engineering and Technology, State Ethnic Affairs Commission, North Minzu University, Yinchuan, 750021, P. R. China.

[c] Ningxia Key Laboratory of Solar Chemical Conversion Technology, North Minzu University, Yinchuan 750021, P. R. China.

*Corresponding authors: sxmin@nun.edu.cn

1. Experimental

1.1 Chemicals and materials

All chemical reagents were used received without further purification unless otherwise noted. The natural basswood used in this study was purchased from the Ruiyi Wood Industry Company (China). Cobalt phthalocyanine (CoPc) and N, N-dimethylformamide (DMF) were purchased from Shanghai Titan Scientific Co., Ltd. High purity carbon dioxide (CO_2, 99.999%) was provided by Beijing Hepu Beifen Gas Industry Co., Ltd. Potassium bicarbonate ($KHCO_3$) was purchased from Aladdin. Ultrapure water (18.2 MΩ cm) was obtained with a Hitech ECO-S15 water purification system.

1.2 Fabrication of CoPc/CWM electrodes

The natural basswood (NW) was first cut into thin slices (2.5 cm×1.5 cm×1.5 mm) perpendicularly to its growth direction. Then, the NW slices were pre-carbonized in air atmosphere at 260 ^{o}C for 6 h with a ramping rate of 5 ^{o}C min^{-1} in a muffle furnace and further carbonized in a tube furnace at 1000 ^{o}C for 6 h under N_2 atmosphere (40 mL min^{-1}) with a ramping rate of 5 ^{o}C min^{-1}. The thus-obtained carbonized wood membrane (CWM) electrodes were carefully polished with 2000 grit sand paper, washed with water, ethanol, and acetone several times with the aid of ultrasonication until no black powder appeared, and dried at 60 ^{o}C in a vacuum oven overnight. Subsequently, the polished CWM electrodes were added into a 6 M HNO_3 solution and refluxed at 80 ^{o}C for 6 h, and then washed repeatedly with ultrapure water, and dried under vacuum overnight at 60 ^{o}C. To prepare the CoPc/CWM electrode, six pieces of acid-treated CWM electrodes (1.5 cm×0.5 cm×0.5 mm) were immersed into 9 mL of DMF containing 2 mg of CoPc. After being ultrasonicated for 1 h and stirred (120 rpm) at 25 ^{o}C for 24 h in a water bath shaking oscillator, the obtained

CoPc/CWM electrodes were collected and washed with DMF three times to remove unabsorbed CoPc, and then dried at 60 °C under vacuum overnight.

1.3 Characterization

Scanning electron microscopy (SEM) images were taken with a ZEISS EVO 10 scanning electron microscope. Transmission electron microscopy (TEM) and high-resolution TEM (HRTEM) images were taken with a FEI Talos F200x field emission transmission electron microscope. X-ray diffraction (XRD) patterns were obtained with a Rigaku Smartlab diffractometer with a nickel filtrated Cu Kα radiation in the 2θ range of 5-80° with a scanning rate of 5° min^{-1}. Raman spectra were collected using a Raman spectrometer (Horiba Evolution) using a 532 nm laser as an excitation source. The specific surface area was determined with the Brunauer-Emmett-Teller (BET) equation at 77 K by using an adsorption apparatus (Micromeritics ASAP 2020 HD 88). X-ray photoelectron spectroscopy (XPS) was performed on a ThermoFisher Escalab-250Xi electron spectrometer using an Al Kα X-ray source. Binding energies were referenced to the C 1s peak (set at 284.4 eV) of the sp^2 hybridized (C=C) carbon from the sample. The loading amount of CoPc was measured by an inductively coupled plasma-optical emission spectrometry (ICP-OES) (Varian 710-ES).

1.4 Electrochemical measurements

All electrochemical measurements were performed on a three-electrode system with a gas-tight two-compartment H-type electrochemical cell. The cathode and anode compartments were separated with a proton exchange membrane (Nafion 117). An Ag/AgCl (with saturated KCl as the filling solution) and a Pt wire were used as reference and counter electrodes, respectively. The as-fabricated CoPc/CWM electrode was soldered to a Cu wire and used as the working electrode (1.0×0.5 cm^2). 0.1 M $KHCO_3$ aqueous solution was used as the electrolyte. Linear sweep voltammetry (LSV) and chronoamperometry measurements were performed using a CHI 660E potentiostat (CH Instruments, Inc., Shanghai, China). All of the applied potentials were measured against an Ag/AgCl reference electrode and converted to the reversible hydrogen electrode (RHE) reference using the equation: E (vs. RHE)=E (vs. Ag/AgCl$_{\text{sat.}}$)+0.5707. The reference electrode calibration was performed in a high purity H_2-saturated electrolyte solution with a Pt wire as the working and counter electrodes, respectively. The LSV measurements were conducted in the potential range of 0.2 V to -1.0 V *vs*. RHE at a scan rate of 1.0 mV s^{-1} after purging the electrolyte with N_2 or CO_2 at least 30 min.

For controlled potential electrolysis of CO_2, CO_2 gas was continuously bubbled into the cathodic compartment at a flow rate of 10 mL min^{-1}. The gas effluent from the cathodic compartment was directly delivered to the gas sampling loop of an online pre-calibrated gas chromatograph (GC, A91 Plus PANNA), which was equipped with flame ionization detector (FID) and thermal conductivity detector (TCD) detectors for analyzing the gas products. At the end of the electrolysis, the liquid-phase products were analyzed by using a high-performance liquid chromatography (HPLC, Hitachi) equipped with C18 column and UV detector (210 nm). A mixed solution of CH_3OH (10 vol%) and phosphoric acid (15 M, pH=2) was used as the mobile phase at a flow rate of 0.6 mL min^{-1}.

The Faradaic efficiencies (FEs) of gas products at each applied potential were calculated by using the volume concentrations detected by the GC as below:

$$FE_i = \frac{2FV_iGtP_0}{RT_0Q_{\text{total}}\times 10^6}\times 100\%$$

The partial current density of CO (J_{CO}) production was calculated using the equation below:

$$J_{\mathrm{CO}} = FE_{\mathrm{CO}} \times J$$

where V_i (vol %) is volume concentration of CO or H_2 in the exhaust gas from the electrochemical cell (GC data) at a given sampling time, G (mL min^{-1}) is gas flow rate at room temperature and ambient pressure, t (min) is electrolysis time, P_0 is pressure (1.01×10^5 Pa), R is the gas constant (8.314 J mol^{-1} K^{-1}), T_0 is temperature (298.15 K), Q_{total} (C) is integrated charge passed during electrolysis (Chronoamperometry data), F is the Faradaic constant (96485 C mol^{-1}).

1.5 Electrochemically active surface area (ECSA) measurement

The ECSA was estimated by measuring the capacitive current associated with double-layer charging from the scan rate dependence of cyclic voltammetry (CV). The measurement was performed among a potential window of -0.13 to -0.23 V *vs.* RHE where the Faradaic current on working electrode is negligible.

2. Additional figures

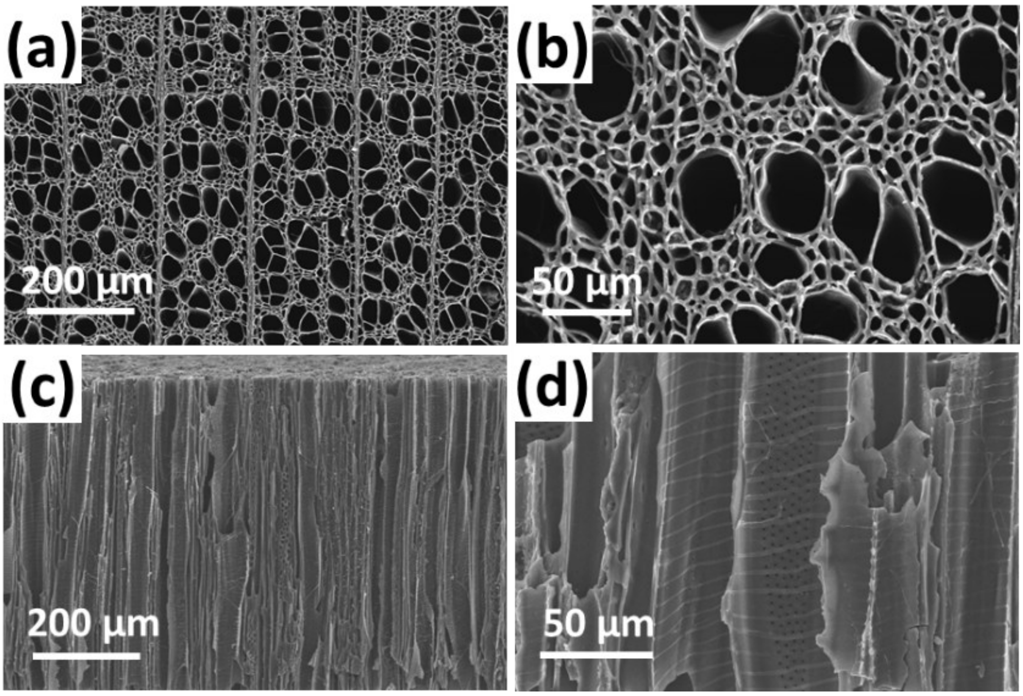

Fig. S1 SEM images of (a, b) top-view and (c, d) side-view of CWM.

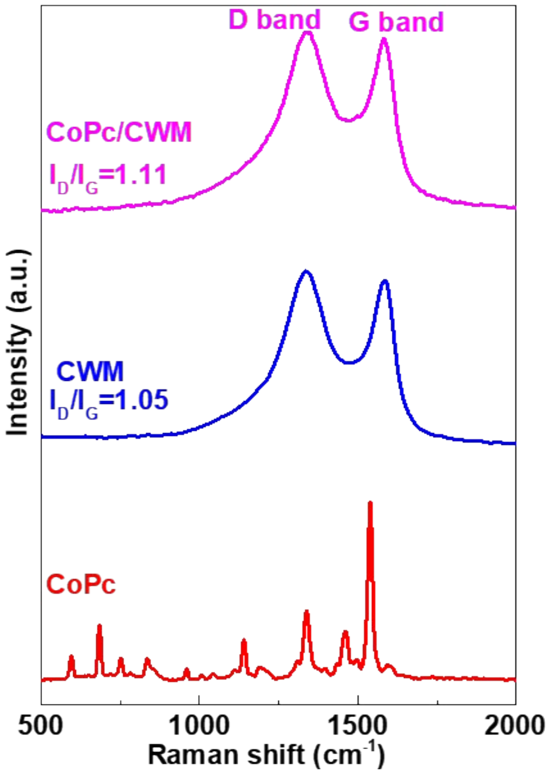

Fig. S2 Raman spectra of CoPc, CWM, and CoPc/CWM electrodes.

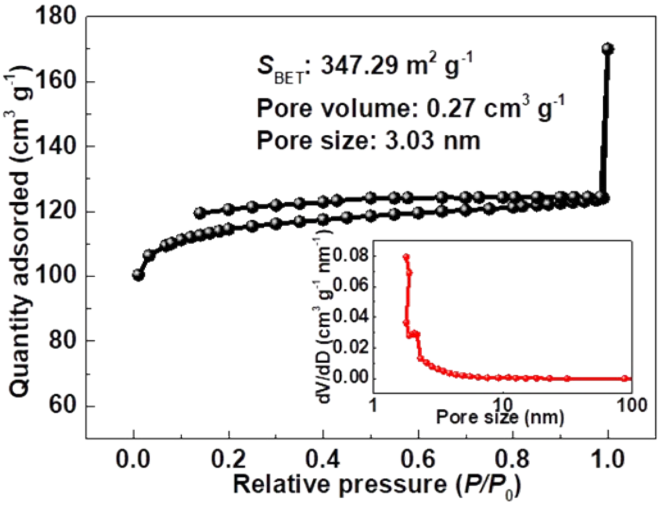

Fig. S3 N_2 adsorption-desorption isotherms and the corresponding pore size distribution (inset) of CoPc/CWM electrode.

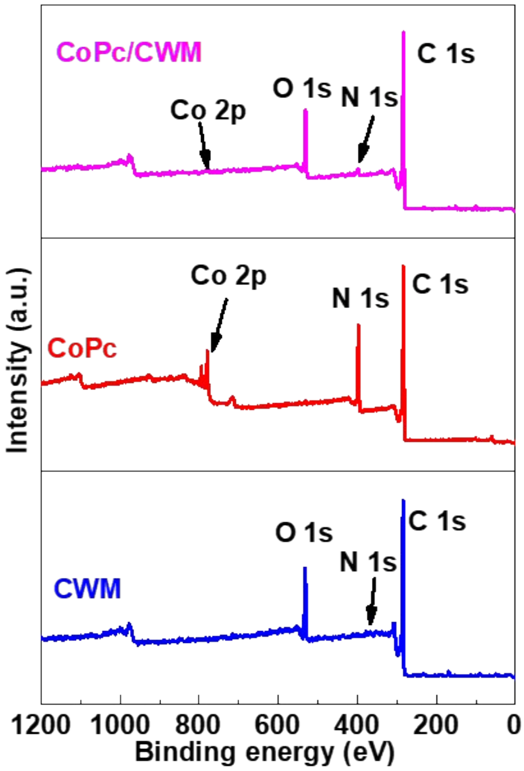

Fig. S4 XPS survey spectra of CWM, CoPc, and CoPc/CWM.

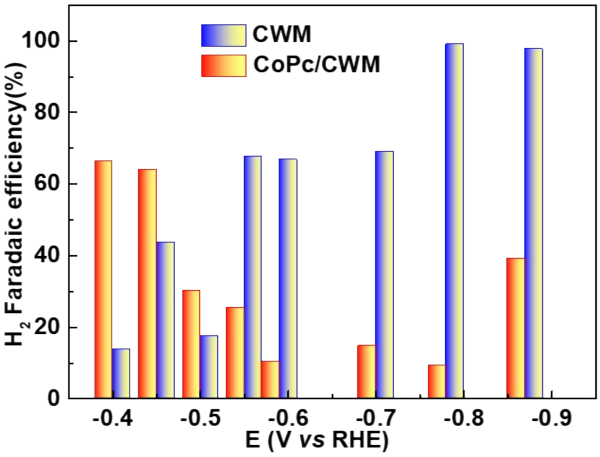

Fig. S5 FE for H_2 production on CWM and CoPc/CWM electrodes at various applied potentials.

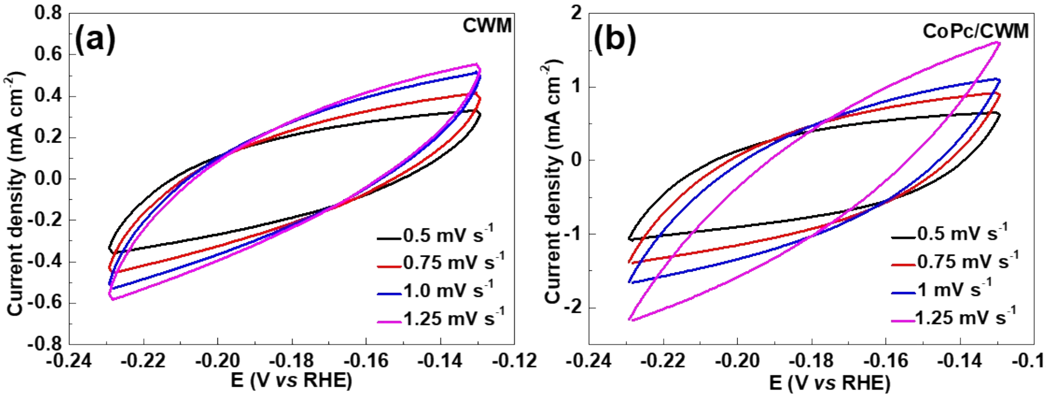

Fig. S6 Cyclic voltammograms (CV) curves under different scan rates for CWM and CoPc/CWM electrodes.

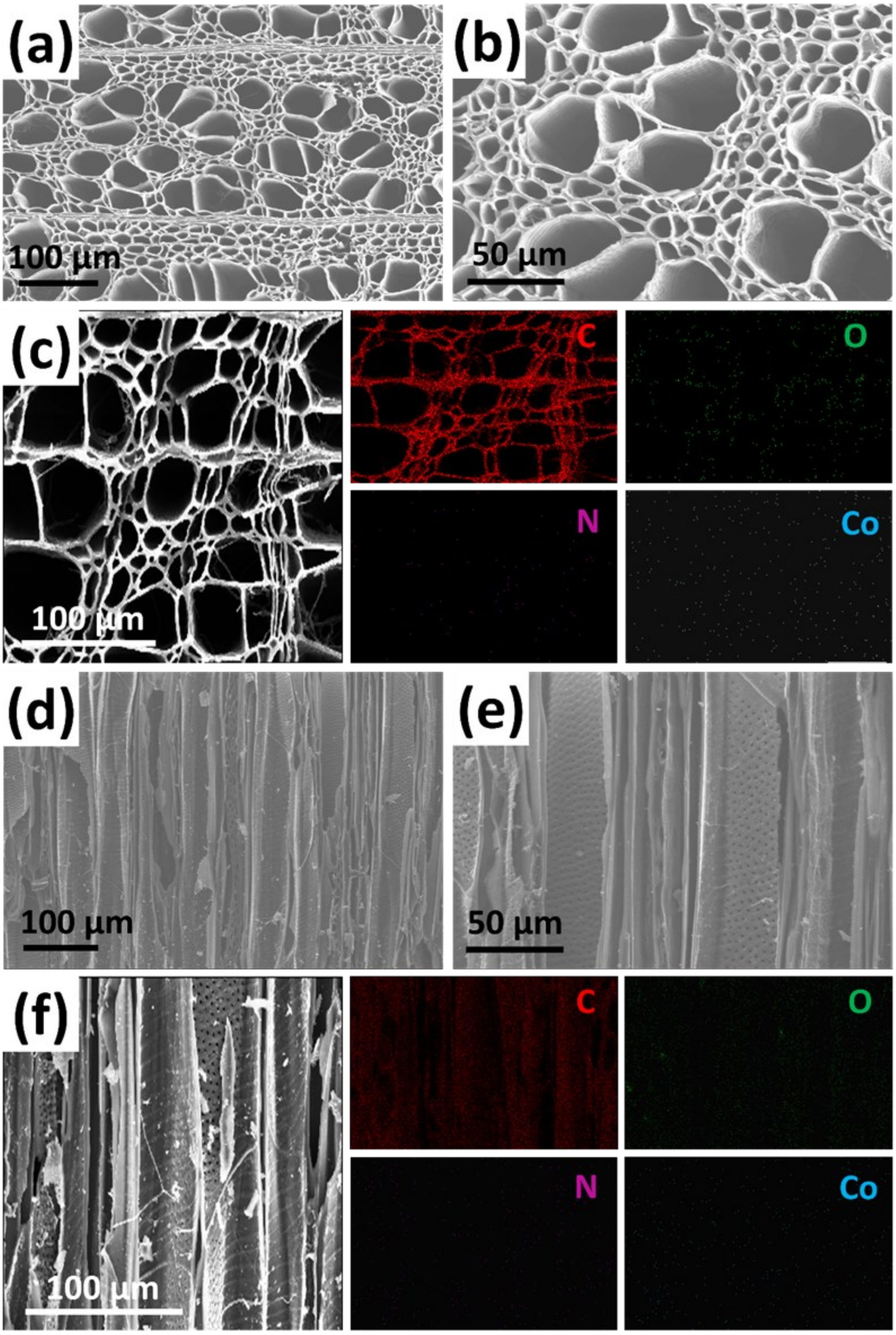

Fig. S7 (a, b) Top-view and (d, e) side-view images of CoPc/CWM electrode after a 12 h of CO_2 reduction electrolysis and (c, f) the corresponding energy-dispersive X-ray (EDX) elemental maps.

Table S1 ICP-OES analysis of CoPc/CWM electrode before and after a 12 h of CO_2 reduction electrolysis

Samples	Mass (g)	Co content (wt%)	Loading of CoPc in CoPc/CWM (mol cm^{-2})
CoPc/CWM	0.0191	0.00446	8.2×10^{-6}
CoPc/CWM after CO_2RR stability	0.0135	0.00202	2.6×10^{-6}

Table S2 Comparison of CO_2RR performances for CO production over reported molecular catalysts.

Samples	Electrolyte	Potential（V *vs.* RHE）	FE CO (%)	CoPc loading (mol cm^{-2})	Ref.
CoPc/CNT	0.1 M $KHCO_3$	-0.63	92	2.4×10^{-5}	1
CoPc-CN/CNT	0.1 M $KHCO_3$	-0.63	98	1.1×10^{-5}	1
CoPc-CN/CNT	0.5 M $KHCO_3$	-0.46	88	1.1×10^{-5}	1
CoPc/OxC	0.1 M $NaHCO_3$	-0.73	94	2.0×10^{-8}	2
6.2-CoPc/ZIS-200	0.5 M $KHCO_3$	-0.83	93	3.0×10^{-4}	3
CoPc-P4VP	0.1 M NaH_2PO_4	-0.73	89	1.3×10^{-9}	4
D-P-CoPc	0.5 M $KHCO_3$	-0.60	97	4.5×10^{-4}	5
CoPc-py-CNT	0.5 M $KHCO_3$	-0.63	98	5.0×10^{-9}	6
N-C-CoPc NR	0.1 M $KHCO_3$	-0.70	85.3	1.5×10^{-6}	7
CoPc/CWM	0.1 M $KHCO_3$	-0.59	90	8.2×10^{-6}	This work

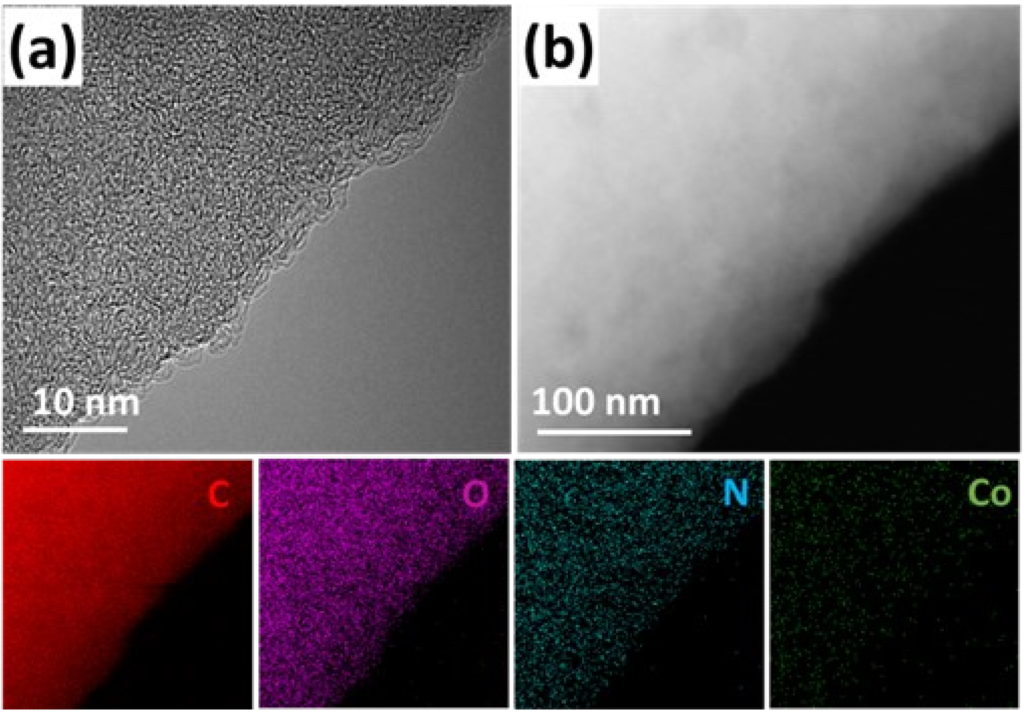

Fig. S8 (a) HRTEM and (b) HAADF-STEM images of CoPc/CWM electrode after a 12 h of CO_2 reduction electrolysis and the corresponding EDX elemental maps.

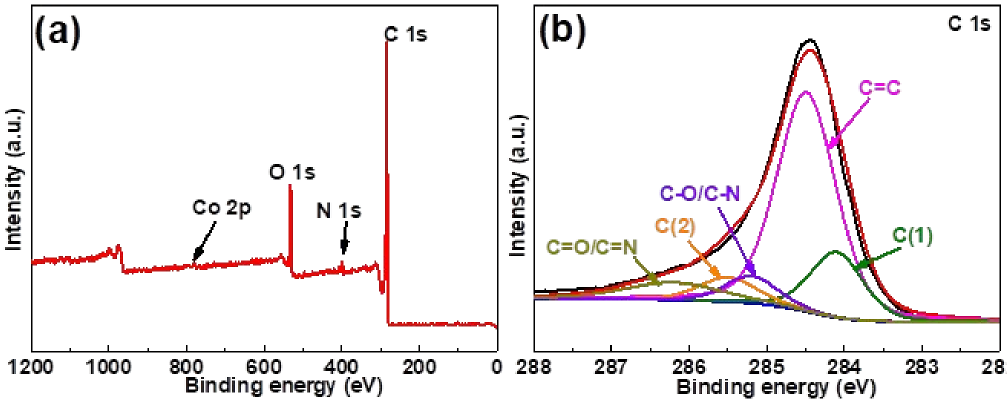

Fig. S9 (a) XPS survey spectrum and (b) high-resolution C 1s XPS spectrum of CoPc/CWM electrode after a 12 h of CO_2 reduction electrolysis.

References

1. X. Zhang, Z. Wu, X. Zhang, L. Li, Y. Li, H. Xu, X. Li, X. Yu, Z. Zhang, Y. Liang and H. Wang, *Nat. Commun.*, 2017, **8**, 14675.
2. M. Zhu, R. Ye, K. Jin, N. Lazouski and K. Manthiram, *ACS Energy Lett.*, 2018, **3**,1381-1386.

3. C. Chen, X. Sun, D. Yang, L. Lu, H. Wu, L. Zheng, P. An, J. Zhang and B. Han, *Chem. Sci.*, 2019, **10**, 1659-1663.
4. W. W. Kramer and C. C. L. McCrory, *Chem. Sci.*, 2016, **7**, 2506-2515.
5. H. Wu, M. Zeng, X. Zhu, C. Tian, B. Mei, Y. Song, X. Du, Z. Jiang, L. He, C. Xia and S. Dai, *ChemElectroChem*, 2018, **5**, 2717-2721.
6. M. Zhu, J. Chen, R. Guo, J. Xu, X. Fang and Y.-F. Han, *Appl. Catal. B Environ*, 2019, **251**, 112-118.
7. H. Zhu, Y. Zheng and M. Shui, *ACS Appl. Energy Mater*, 2020, **3**, 3893-3901.